Polarization-Dependent Gain in SOA-Based Optical Multistage Interconnection Networks

Odile Liboiron-Ladouceur, *Student Member, IEEE*, Keren Bergman, *Member, IEEE*, Misha Boroditsky, *Senior Member, IEEE*, and Misha Brodsky, *Member, IEEE*

***Abstract*—The small polarization dependence (< 1 dB) of optical components becomes significant in optical multistage interconnection networks. The cumulative effect can ultimately limit physical layer scalability by changing the maximum number of internal nodes that optical packets can traverse error free. It is shown that for nodes based on commercial semiconductor optical amplifier (SOA) switches with polarization-dependent gains of less than 0.35 dB, the maximum number of cascaded nodes changes by as much as 20 nodes, depending on both the packet wavelength and its state of polarization. This deviation in the number of nodes could correspond to a 100-fold decrease in the number of interconnected ports of an optical interconnection network such as the data vortex. This dramatic effect is explained in terms of optical signal-to-noise ratio degradation due to accumulated amplified spontaneous emission noise originating from the SOA device in the node.**

***Index Terms*—Multistage interconnection networks (MINs), optical packet switching, polarization-sensitive devices, semiconductor optical amplifier (SOA).**

I. Introduction

OPTICAL packet-switched (OPS) multistage interconnection networks (MINs) are a promising means of routing high-bandwidth optical data messages with low communication latency [1]. Through dense wavelength-division multiplexing (DWDM) technology, optical interconnection networks offer the potential to address the need for throughput scalability while maintaining low latency [2]. Depending on the network size, the applications can range from local area and storage networks to high-performance computing [3]. Several research groups have proposed and investigated different OPS network topologies in a recent JOURNAL OF LIGHTWAVE TECHNOLOGY special issue [4]. Most notably, the data vortex network architecture has been shown to be a particularly attractive candidate as a multiple-wavelength OPS network that is capable of scaling in both the network size and packet bandwidth [5].

Manuscript received April 3, 2006; revised July 28, 2006. This work was supported in part by the National Science Foundation under Grants ECS-0322813 and ECS-0532762 and by the U.S. Department of Defense under Subcontract B-12-664.

O. Liboiron-Ladouceur and K. Bergman are with the Department of Electrical Engineering, Columbia University, New York, NY 10027 USA (e-mail: ol2007@columbia.edu; bergman@ee.columbia.edu).

M. Boroditsky was with AT&T Laboratories, Middletown, NJ 07748 USA. He is now with Knight Equity Markets, Jersey City, NJ 07310 USA (e-mail: mboroditsky@knight.com).

M. Brodsky is with AT&T Labs Research, Middletown, NJ 07748 USA (e-mail: brodsky@research.att.com).

Digital Object Identifier 10.1109/JLT.2006.883122

In most OPS networks, the predominant switching element is the commercially available semiconductor optical amplifier (SOA), due to its broad gain bandwidth, fast switching, and potential for integration [6]–[8]. In the data vortex architecture, SOAs transparently route individual packets that contain multiple wavelength-division multiplexing (WDM) payload channels. Aside from acting as a gating switch, the SOA compensates for the optical power losses from the passive optical components of the node structure (e.g., couplers, delay lines, and connectors). The performance and scalability of SOA-based OPS networks have been investigated for a range of architectures [7], [9], [10], without necessarily considering the effect of the component's polarization dependence. The inherent polarization-dependent gain (PDG) of the SOA, albeit very small in modern devices [11], [12], accumulates as the packets propagate through a cascade of SOA-based nodes and affects the overall system performance. In fact, we observed, in our previous studies of optical packets propagation carrying eight 10-Gb/s WDM channel payloads, that packet polarization influences the node cascadability even when using commercial SOAs with very low PDG [10]. The origin of PDG in SOAs is the fact that bulk active material has much larger transverse electric (TE) amplification than transverse magnetic (TM), which is due to the different confinement factors [11]. To compensate for the birefringence, the strain in the active material enhances the gain of TM with respect to TE, making the SOAs less polarization dependent. However, this balance does not entirely mitigate PDG and is dependent on input power, gain, and wavelength. In addition to the cumulative effect of PDG, the SOAs also introduce amplified spontaneous emission (ASE) noise, which affects the optical signal-to-noise ratio (OSNR) of the payload channels. The gain will also vary with wavelength for multiple propagated DWDM channels. Signal degradation due to these effects increases with the number of cascaded nodes.

In this paper, we discuss in Section II the source of PDG in an OPS network and the difficulty in determining its effect within MIN topologies such as the data vortex. We then study the impact of cumulative PDG by sending packets through a virtual cascade of SOA-based nodes using a recirculating loop, as described in Section III. By setting two polarization controllers (PCs), one inside the recirculating loop and one at its input, we control both the input state of polarization (SOP) and the PDG accumulation of each traversed loop. In Section IV, small node PDG is measured by maximizing the PDG accumulation in the loop. In Section V, we characterize the network performance by taking the bit error rate (BER) measurements as a function of

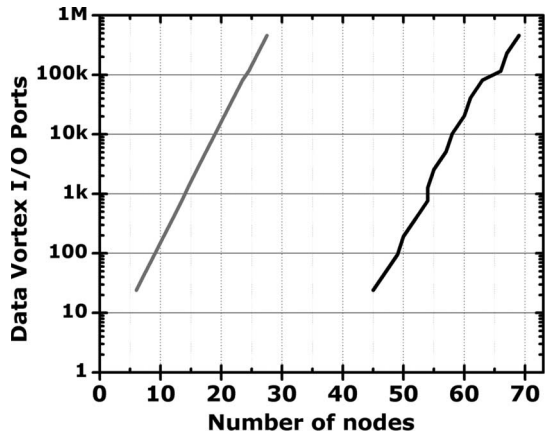

Fig. 1. Data vortex I/O port size versus the number of nodes under heavy load. Network size for the median number of hops (gray) and for 99.999% of the injected packets (black).

the number of cascaded nodes for three different wavelengths. For two extreme cases of maximum and minimum cumulative PDGs, we observe the wavelength-dependent variations in the number of nodes through which packets could travel error free. We show that in all cases, an increase in the BER arises from the OSNR degradation due to accumulated ASE noise. Finally, we discuss possible PDG compensation approach, which minimizes the effect of cumulative PDG in an OPS network.

II. PDG in Multistage Networks

A. Multistage SOA-Based Network

In a MIN, packets propagate through a cascade of switching nodes before reaching their destination. In general, a greater number of switching nodes corresponds to a larger input and output port count, which is proportional to $\log_2(N)$ for an $N \times N$ port network. In the data vortex, the number of nodes through which a packet will propagate is nondeterministic. Simulations of the data vortex as a large-scale switching fabric have shown that for a heavily loaded data vortex implementation with 10 k $\times$ 10 k ports, 99.999% of the injected packets propagate through fewer than 58 internal switching nodes (Fig. 1). The non-Gaussian distribution curve exhibits a median of 19 cascaded nodes. The asymmetric distribution is due to deflection-based contention resolution, where a packet is rerouted, preventing collisions with other packets. Deflecting packets eliminates the requirement for buffers but increases the path length by two switching nodes per deflection. Due to the distribution profile of the number of nodes in a packet's path, the cumulative effect of node polarization dependence becomes statistically difficult to assess on a packet-by-packet basis. Additionally, the SOP of each channel within the multiple DWDM packet structure will rotate at a different rate due to polarization mode dispersion (PMD). These effects, combined with ASE accumulation and wavelength-gain dependence from the SOA devices, increase the complexity in properly designing optical multistage networks. It is therefore important to determine the impact of cumulative PDG itself to determine the appropriate margins in the physical layer.

B. PDG of an SOA-Based Switching Node

The switching nodes within the data vortex architecture are based on conventional fiber-optic technologies. The simple switching node structure is shown in Fig. 2(a). Each node has two input ports and two output ports. The input packet is directed to one of the two output ports through couplers. The payload data in the packet are encoded on multiple DWDM channels in parallel with the header- and frame-signal wavelengths [Fig. 2(b)]. In a time slot, one packet is processed within each node and routed based on the destination address encoded in the header signal. A small portion of optical power is tapped off, and the header and frame bit information is filtered and converted into an electrical signal to turn on one of the two SOAs. During the routing decision processing, the payload data are delayed in a small length of fiber. The internal node is transparent to the payload data since the output power of each payload channel equals its input power. In this investigation, a programmable pattern generator makes the routing decisions. This is the basis by which a virtual network is created where the packets can be routed through the same switching node. The two SOAs are InGaAsP/InP tensile-strained bulk devices from Kamelian (OPS-10-10-X-C-FA), which were specified to have a noise figure of 7.0 dB and a saturation input power of approximately -2.5 dBm for an injection current of 40-mA. The SOA operates in the linear regime with a gain of 6.5 dB, compensating for the losses of two couplers and connectors in the node. The SOA-device PDG specifications are 0.52 dB at 1528 nm and 0.10 dB at 1550 nm at a gain of 13 dB. The maximum PDG measured is 0.5 dB for the SOA settings in the switching node. The polarization-dependent loss (PDL) of the couplers, the fiber, and the connectors is insignificant compared to the PDG of the SOA devices. We therefore refer to the PDL and PDG of the node as simply node PDG.

III. Experimental Setup

A. Controlling the Polarization of a Virtual Network

A schematic of the recirculating loop used in this investigation is shown in Fig. 3. Three cooled distributed-feedback lasers emitting at 1531.05, 1543.2, and 1553.82 nm, respectively, are used to investigate the PDG over the SOA-gain bandwidth. The channels are multiplexed into a single fiber and modulated simultaneously with a dual-drive Mach–Zehnder modulator at 10 Gb/s. The modulator is driven by a nonreturn-to-zero pseudorandom bit sequence with a length of $2^9 - 1$, which was produced by the fast pattern generator (PPG1). A short packet of 25.6 ns is created using a separate SOA to gate the continuous data stream. The launched SOP of the payload channels is set using a PC (PC Input).

The loop contains one SOA-based switching node such as the one described in the previous section that was used in the data vortex OPS interconnection network. The recirculating loop is created by connecting one of the node outputs to its input using a fiber. Packets are either routed back to the same node through a 40-ns-long loop or out of the loop. The corresponding fiber length of a few meters makes this type of recirculating loop different from the conventional loop used to

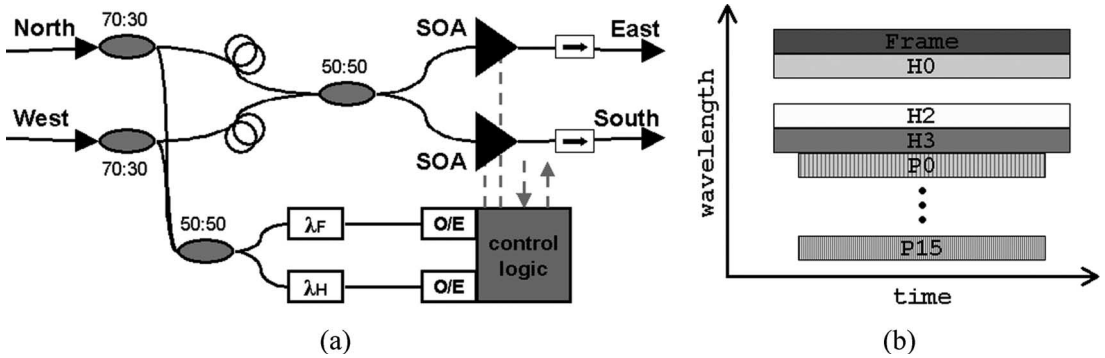

Fig. 2. (a) Switching node configuration of the data vortex. (b) Multiple DWDM channel packet structure.

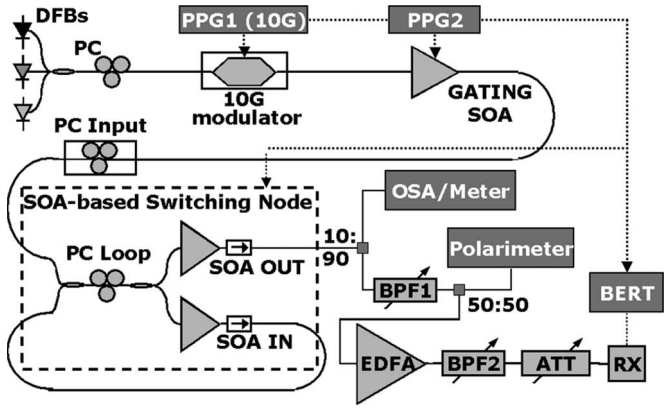

Fig. 3. Recirculating loop (PPG, pulse pattern generator; SOA, semiconductor optical amplifier; EDFA, erbium doped fiber amplifier; BPF, bandpass filter; RX, burst-mode optical receiver module; PC Input, PC to change the input SOP; PC Loop, PC to change the node PDG; OSA, optical spectrum analyzer). Optical path (solid line) and electrical path (dashed line).

investigate WDM transmission systems, where gain elements are usually separated by kilometers [13]. The header and frame information is not transmitted along with the packet; instead, a programmable pattern generator (PPG2) sends a switching signal, bypassing the optical-to-electrical conversion, and the routing control logic gates. The modification is suitable since the measurement addresses the number of nodes traversed by the packets, assuming proper routing logic function. Two PCs adjust the PDG of concatenated loops (PC Loop) included in the switching node and the input SOP (PC Input). In this configuration of the switching node, the SOAs operate in the linear regime with a gain of 6.5 dB to compensate for the losses of the two couplers and connectors in the node.

A single packet is injected into the loop through one of the node's ports with a period of 3.2 μs (80 loop roundtrips) to ensure that there is at most one packet in the loop at a time. After a predetermined number of loops that corresponds to the desired number of cascaded nodes, the packet drops out of the loop through the other SOA at a selected time interval. To increment the number of nodes by one, the control signal to "SOA OUT" is delayed by 40 ns, which corresponds to one loop length.

At the output of the recirculating loop, 10% of the packet optical power is used to measure the OSNR of each payload channel using an optical spectrum analyzer (OSA; dB/0.1 nm resolution). The first stage of the packet receiver system measures the channel's OSNR as a function of the number of cascaded nodes. Additionally, the total optical packet power is measured by replacing the OSA with an optical power meter to monitor power saturation in the loop due to the ASE, which accumulates as packets propagate through multiple cascaded nodes. The total packet power is important to monitor to determine if the SOA reaches saturation. Nonlinearities in saturated SOAs can affect the performance results. The second stage of the packet receiver system consists of measuring parameters specific to the channel under investigation. A bandpass filter (BPF1) initially filters the payload channel. The channel is then divided, with half of the signal power used to monitor its SOP with a polarimeter (HP 8509). This is to ensure full coverage of the Pointcaré sphere in the methodology used to measure the impact of cumulative PDG. The other half of the signal is used to perform BER measurements on the data payload. The signal is optically preamplified with an erbium-doped fiber amplifier (EDFA) and filtered again (BPF2) to remove the out-of-band ASE noise [14]. A burst-mode optical receiver (RX), which consists of a dc-coupled 10.7-Gb/s p-i-n that is integrated with a transimpedance amplifier and a limiting amplifier, digitizes the data payload in the channel. Prior to the receiver, an attenuator (ATT) sets the optimum optical power incident on the p-i-n of the optical receiver module. A BER tester receives an external gating signal synchronized to PPG1 and PPG2 and counts cumulative errors on the data payload of incoming packets while ignoring the dead time between packets. The gating signal is a 20-ns pulse centered in the middle of the 25.6-ns-long packet to frame the measurement of valid data outside the rise and fall times. This front-end receiver has a measured sensitivity of -35 dBm (BER $< 10^{-9}$). Through the two stages of the packet receiver system, a complete understanding of the impact of cumulative PDG on each payload channel in terms of their optical average power and OSNR is achieved.

IV. Cumulative PDG

A. Extreme Cases of Cumulative PDG

Minimizing and maximizing the PDG accumulation in the loop in a controllable fashion can accurately measure the effect of relatively small PDG of the switching node on the network physical layer scalability. The SOP is a vector that will experience rotation as it propagates through the SOA devices [15]

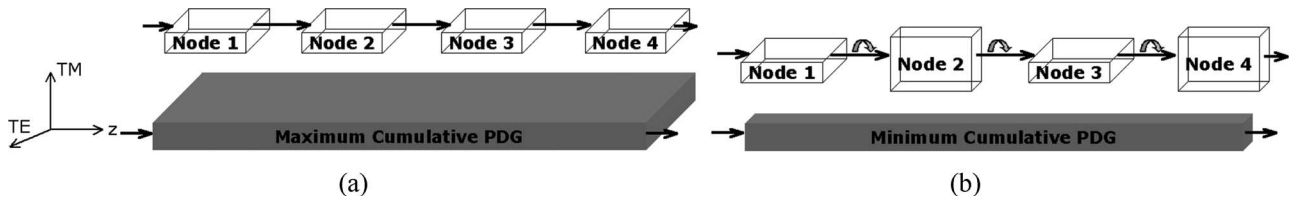

Fig. 4. Conceptual illustration of (a) maximum cumulative PDG and (b) minimum cumulative PDG.

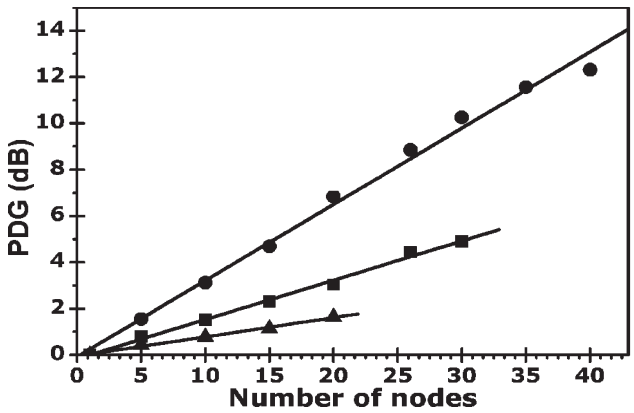

$$\left|\overrightarrow{PDG_{node}}\right| = \left|P_{\max} - P_{\min}\right|$$

$$\overrightarrow{PDG_{Network,\max}} = \sum_{nodes=1}^{N} \overrightarrow{PDG_{node}}$$

Fig. 5. Maximum PDG increasing linearly for channels at 1531.05 (circle), 1543.29 (square), and 1553.82 nm (triangle).

and the other elements of the switching node. The cascade of multiple nodes will correspond to a total PDG that will affect the OSNR and average power of the payload channels. The mechanical PC inside the loop (PC Loop) allows the vector to be aligned in a specific way to either maximize or minimize the cumulative PDG (Fig. 4). Neither of those two extreme cases is likely to occur in a real network. Statistical analysis can be performed to assess the likelihood of the amount of cumulative PDG based on the number of concatenated polarization-dependent elements [16]. However, it becomes cumbersome to determine the physical layer scalability of a network in terms of the number of ports and internal switching nodes when additional signal degradation occurring at the nodes needs to be included in the statistical behavior of the PDG. The recirculating loop allows us to establish the scalability limits by isolating cumulative PDG effects in an optical MIN topology such as the data vortex.

By controlling the polarization in the recirculating loop, we investigate three different cases of the impact of PDG on each of the three payload channels to quantify the effect of PDG on multichannel packets. For the first two cases, the PC Loop is adjusted such that the channel's polarization returns to the same state after one loop trip [Fig. 4(a)]. The channel's input SOP corresponding to the lowest gain monitored is referred as the "Low Gain" case, while the one corresponding to the highest gain is referred as the "High Gain" case. The third and final case corresponds to the "No PDG" case, where the PC Loop is set to change the packet's polarization to the orthogonal one as it travels through one loop so that the PDG of consecutive loops cancel each other such that practically no cumulative effect is observed [Fig. 4(b)]. Due to the small but finite PMD in the deflection fiber, these three PC Loop settings are channel specific. To adjust the PC Loop in one of the three settings for the three channels, the PDG is measured by monitoring one channel power at the output of the loop while the PC Input operates in a scrambler mode covering the entire Pointcaré sphere for that same channel under measurement. The measurements are repeated for the two other channels by appropriately adjusting the PC Loop.

B. Single SOA-Based Node PDG

The methodology of concatenating multiple nodes allows for accurate measurements of relatively small polarization dependences of one node when the cumulative PDG is maximized. The node PDG corresponds to the rate of increase in the power differences between the High Gain and Low Gain cases with respect to the number of nodes (Fig. 5). In this case, the PDG effect is maximized, and it accumulates in a linear fashion as the packet traverse consecutive loops.

Clearly, the measured node PDG is wavelength dependent with 0.33 dB at 1531.05 nm, 0.17 dB at 1543.29 nm, and 0.09 dB at 1553.82 nm for an SOA gain of 6.5 dB. As previously mentioned, the SOA device specifications show similar wavelength dependence with 0.52 dB at 1528 nm and 0.10 dB at 1550 nm at a gain of 13 dB. Higher PDG is associated with higher gain, as the balance achieved between the differences in confinement factors and the strain in this particular SOA design is more difficult to maintain at high gain [17]. In a real system, the cumulative PDG will oscillate between the minimum and maximum gains with the number of nodes, due to the structure of the recirculating loop [18], [19].

V. Network Physical Layer Scalability

A. Power Evolution of Payload Channels

In Fig. 6(a), the measured optical power of each of the three payload channels is plotted as a function of the number of

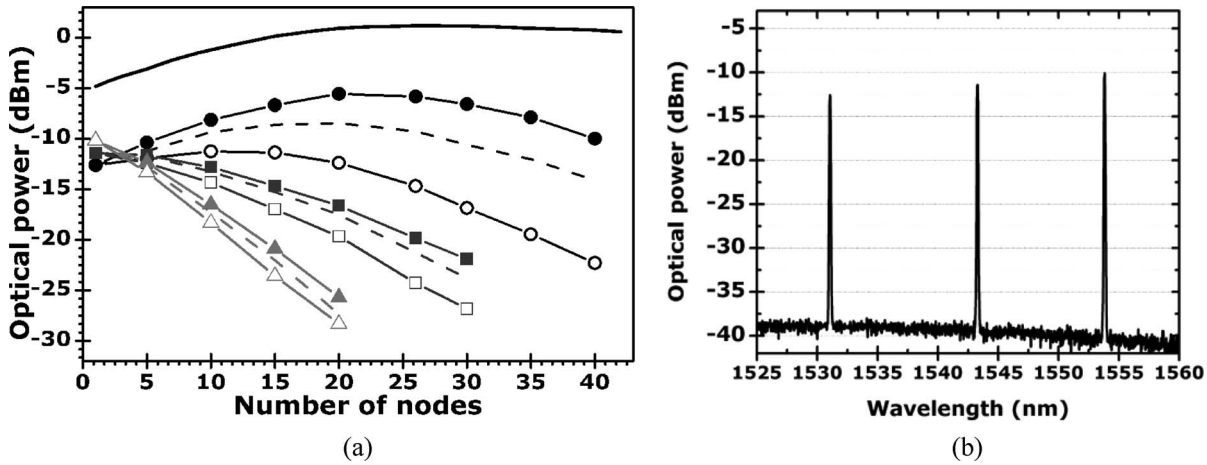

Fig. 6. (a) Optical power as a function of the number of cascaded nodes for High Gain (solid symbols), Low Gain (open symbols), and No PDG (dashed lines) at 1531.05 (circle), 1543.29 (square), and 1553.82 nm (triangle). The plain line represents the total power of the packet. (b) Average optical power of the three payload channels with some preemphasis.

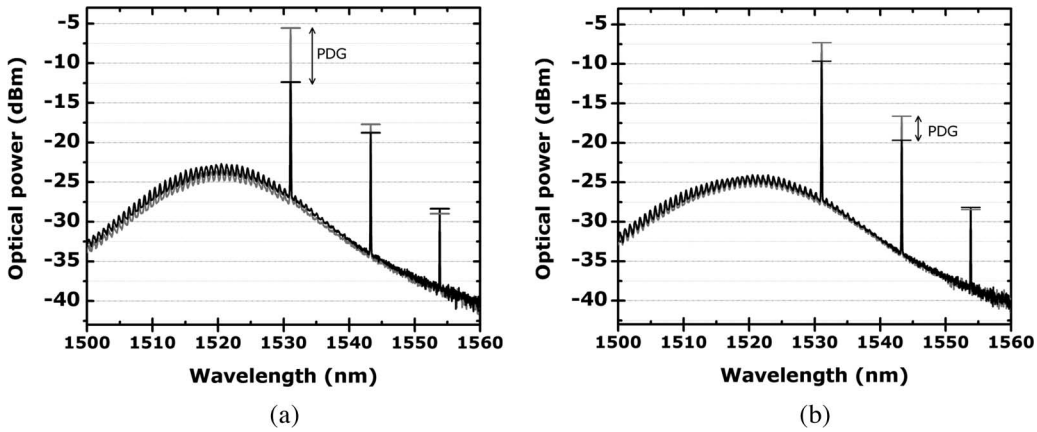

Fig. 7. Output spectrum for the Low Gain case (black) and the No PDG case (gray) after 20 hops for the channel at (a) 1531.05 and (b) 1543.29 nm. The vertical markers indicate the power of the three channels.

nodes propagated for all three cases: High Gain, Low Gain, and No PDG. Preemphasis in the input power of the three payload channels compensates for the effect of the wavelength gain dependence of the SOA devices [20]. The average optical power is shown in Fig. 6(b) with −12.5, −11.0, and −10.0 dBm for 1531.05-, 1543.29-, and 1553.82-nm channels, respectively. For some channels, the node transparency is broken by the combined effects of PDG, PDL, and the wavelength-dependent gain of the components of the node. When this occurs, as shown in Fig. 6(a), for channels at 1543.29 and 1553.82 nm, the packet experiences a net loss that travels through the cascade of nodes. Concurrently, for the channel at 1531.05 nm, the minimum and maximum powers change in a nonlinear fashion and saturate after an initially linear increase. The total optical power of the multiwavelength packet at the output of the loop indicates a shift in the SOA operating regime from linear to saturation after 20 nodes. There is a delicate balance between ensuring adequate gain for the longer wavelength channels and maintaining the shortest channel in the linear regime to prevent nonlinearity effects from degrading the signal.

The output spectrum of the extracted packet after 20 nodes is shown in Fig. 7 for the maximum cumulative PDG for channels at 1531.05 and 1543.29 nm. In a real network system, the channel's power lies between the Low Gain and High Gain cases with a statistical probability [16]. In Fig. 7(a), the two other channels' powers vary by a small amount compared to the power of the channel for which cumulative PDG is maximized. Therefore, the power of the channel at 1531.05 nm fluctuates less compared with the power of the channel at

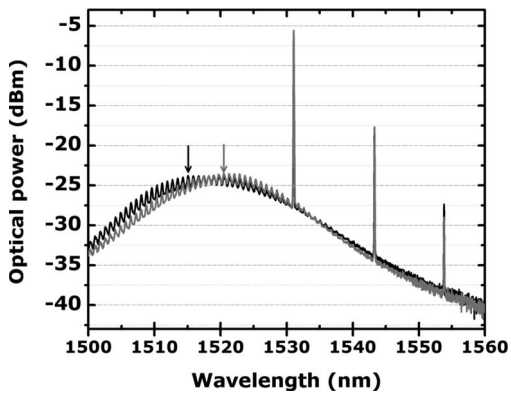

Fig. 8. Output spectrum for the case of maximized PDG (gray) and minimized PDG (black) for the channel at 1531.05 nm after 20 nodes, with two arrows pointing at the corresponding peak ASE.

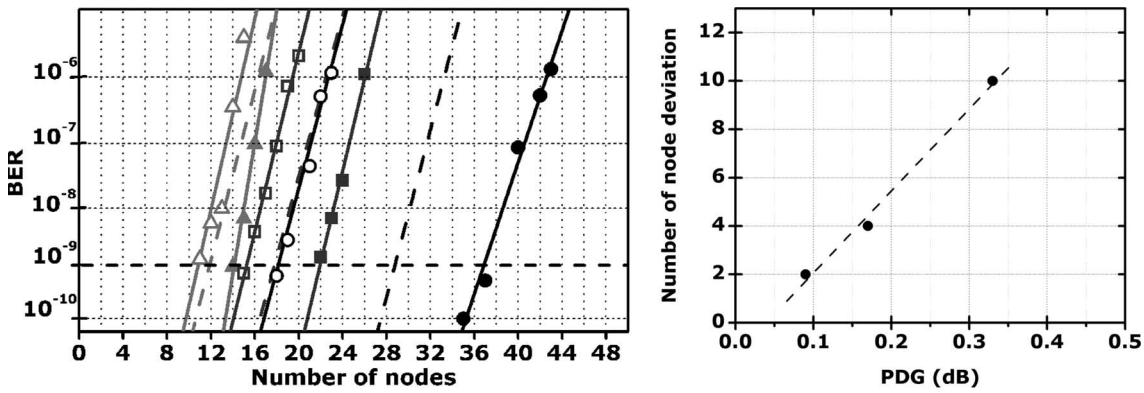

Fig. 9. (a) BER measurements for the channel at 1531.05 (circles), 1543.29 (square), and 1553.82 nm (triangle) for the High Gain (solid symbols), Low Gain (empty symbols), and No PDG cases (dashed lines). (b) Number of node deviation from the case of No PDG versus PDG.

1543.29 nm, for which the cumulative PDG was maximized [Fig. 7(b)]. The fiber PMD makes each channel of the packet rotate at a different rate such that the required PDG alignment only holds for one wavelength. When the cumulative PDG is minimized, the peak wavelength of ASE shifts by 5.4 nm, from 1520.49 to 1515.09 nm, when the cumulative PDG is maximized (Fig. 8). For this SOA design, a peak ASE at shorter wavelengths corresponds to lower PDG [20]. Interestingly, minimizing the cumulative PDG has the effect of shifting the peak ASE noise to the left, i.e., to a shorter wavelength. The small ripples on the curves in the spectra are the residual reflectivity on the SOA facets.

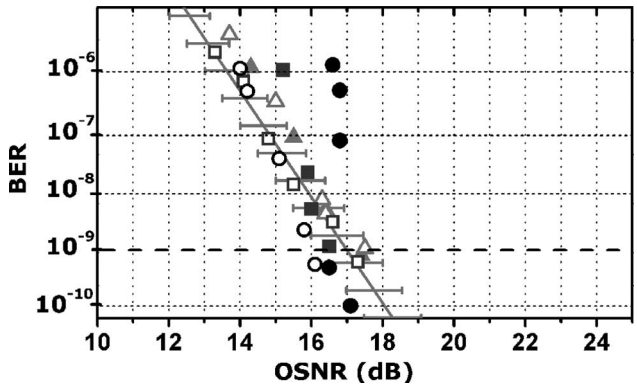

Fig. 10. OSNR versus BER measurements: Back-to-back receiver sensitivity range (gray lines) and for the three payload channels for High Gain (solid symbols) and Low Gain (empty symbols).

B. Maximum Reach

We can now turn to an investigation of the impact of the cumulative PDG on network size scalability. For each channel, three BER curves (corresponding to the three cases of High Gain, Low Gain, and No PDG) are taken as a function of the number of cascaded nodes through which a packet propagates (Fig. 9). The performance metric used to quantify the impact of the node PDG on the size of the multistage network is the maximum number of cascaded nodes propagated by a packet while maintaining a BER below 10^{-9}. At 1531.05 nm, this number varies by almost 20 nodes, from 18 cascaded nodes in the Low Gain case to 37 cascaded nodes in the High Gain case. These two limits deviate by about 10 nodes from the case of No PDG. Similarly, the performance of the channel at 1543.29 nm ranges by seven nodes, from 15 to 22 nodes, deviating by about four nodes from the No PDG case. Thus, large deviations in the maximum allowable cascaded nodes associated with the presence of even small individual node PDG can profoundly affect the network scalability when the PDG is not carefully considered. In a large data vortex network of 10 k $\times$ 10 k ports, the shortcoming in performance by 10 cascaded nodes less than projected corresponds to a network size reduction factor of 100 down to a 100×100 port network. Based on these data, we conclude that appropriate channel placement in the region of lower PDG (1553.82 nm instead of 1531.05 nm) could significantly improve network performance uniformity. The lower gain associated with lower PDG makes this approach most applicable to smaller networks in the order of 100 ports or less. In Fig. 9(b), the deviation from the case of No PDG is plotted as a function of the node PDG of the channel's wavelength. The network spread exhibits a linear relation, with the amount of node PDG increasing at a striking rate of approximately 34 node/1 dB of PDG.

For each point of the data set in Fig. 9, the OSNR was measured in addition to the BER. These OSNR measurements are plotted as a function of the corresponding BER in Fig. 10. The back-to-back receiver sensitivity to the payload channel's OSNR is 17 $\pm$ 0.7 dB at a BER of 10^{-9} for all three wavelengths, which is indicated by the gray line with error bars on the plot. Most data points lie within the sensitivity limitation of the receiver. Hence, we conclude that the impact of cumulative PDG can be largely described as OSNR degradation for each wavelength. In the presence of PDG, the additional gain seen by some SOP could create some node gain overcompensation, which extends the lifetime of the packet in the network. Alternatively, the gain reduction for some SOP could cause degradation of the channel OSNR due to ASE noise.

The additional OSNR penalty for some of the data points outside the OSNR receiver sensitivity is ascribed to nonlinear effects as the SOA reaches saturation. These points (three black circles) correspond to the 40-, 42-, and 43-node propagations by the shortest wavelength channel (1531.05 nm). As

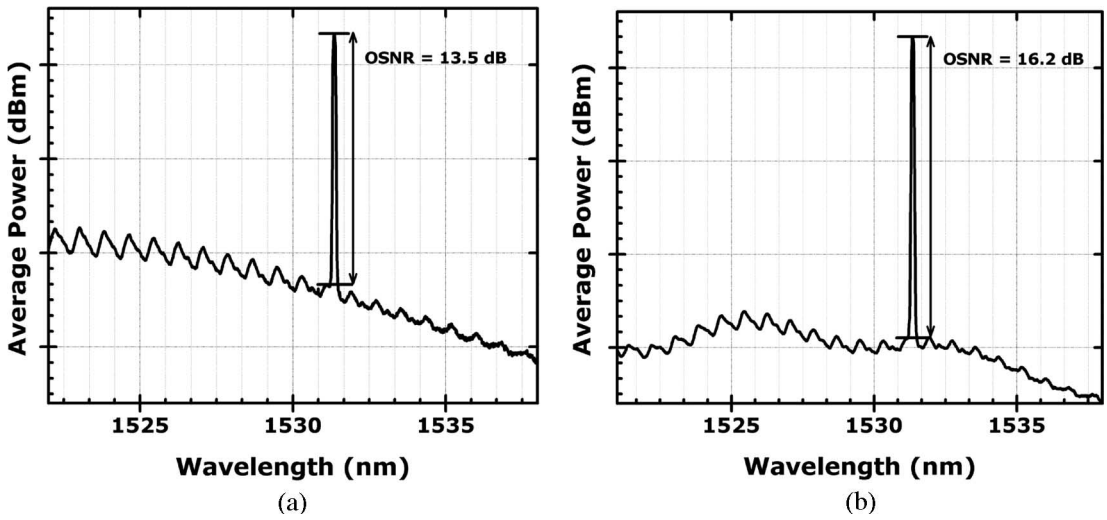

Fig. 11. Spectra of the shortest wavelength channel (1531.05 nm) (a) before and (b) after use of the PC and linear polarizer, showing evidence of partially polarized noise for the High Gain case after 20 cascaded nodes.

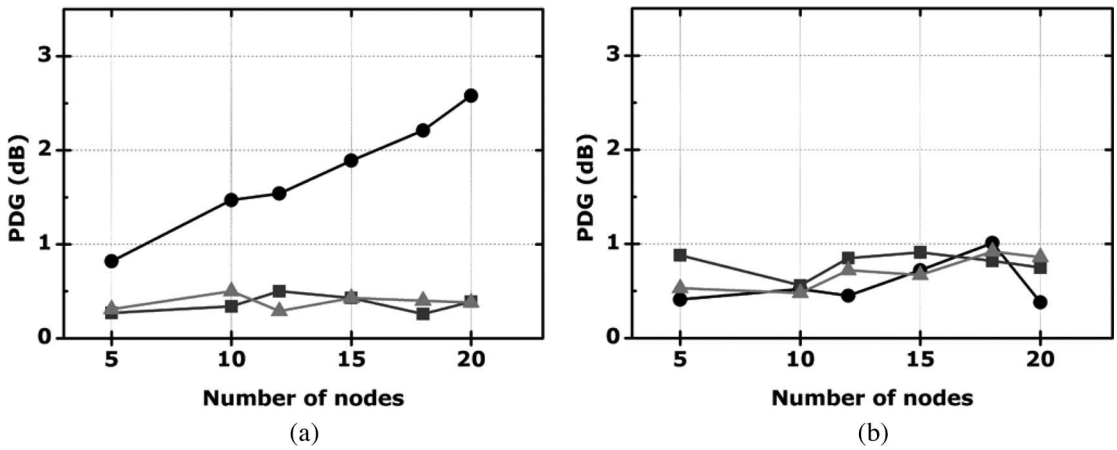

Fig. 12. Cumulative PDG for all three payload channels when the PC Loop is set to minimize PDG for the channel at (a) 1543.29 nm after 20 nodes and (b) 1531.05 nm after 20 nodes.

the packet propagates through a greater number of cascaded nodes, the SOA operates in a heavily saturated regime. The shortest channels experience spectral broadening due to gain-saturation-induced self-phase modulation [21], which degrades BER performance. Interestingly, partially polarized noise possibly causes lower OSNR requirements for the other points outside the receiver sensitivity, which correspond to 35- and 37-node propagations (two black circles) and to 18-node propagation (white circle). At the receiver, the signal-noise beating is polarization sensitive, and half of the noise beats with the signal in a system with unpolarized noise. In the High Gain case of our investigation, the shortest channel has sufficient gain to propagate through a greater number of cascaded nodes than the other channels. The channel's signal and the noise become partially polarized [22]–[24]. To verify if the noise is indeed partially polarized, OSNR measurements are performed using a PC, and a linear polarizer is inserted at the output of the loop. After propagating through 20 cascaded nodes, the SOP of the shortest channel is aligned to the linear polarizer using the PC. The measured OSNR is 16.2 dB, which is 2.7 dB higher than that in the absence of the PC and polarizer (Fig. 11). Evidently, more than half of the SOP of the noise is orthogonal to the SOP of the signal, affecting the unique performance relation between the OSNR and BER of an unpolarized system.

C. Minimizing Cumulative PDG

The effect of cumulative PDG on the OSNR of the channels can be minimized through the SOA devices that exhibit a PDG of less than 0.1 dB. Alternatively, optimized channel placement can be considered for smaller network sizes. For larger network sizes, PDG compensation techniques are necessary to minimize the dramatic shift in performance. In the recirculating loop, the PC Loop is set to compensate for the node PDG at one channel while monitoring the other channels. In Fig. 12(a), the channel at 1543.29 nm is compensated, but the channel at 1531.05 nm still experiences significant PDG accumulation. When compensation is done for the channel at 1531.05 nm [Fig. 12(b)], the cumulative PDG for the channels at 1543.29 and 1553.82 nm remain under an acceptable limit (< 1 dB), which corresponds to a minimum node deviation in the number of cascaded nodes. In a realistic network, this type of compensation is technically

possible but requires monitoring the SOP of the channels over time and adjusting the PC. In a MIN with one PC at each internal switching node, this technique quickly becomes impractical. However, the measurement indicates that the PDG effect can be minimized by using polarization-maintaining (PM) fiber and couplers between internal nodes. Each wavelength channel should be linearly polarized and launched such that the SOP coincides with the slow axis of the PM fiber. The PM fiber polarization axis should then be aligned to the SOA's waveguide such that the birefringence is compensated for channels that experience higher PDG. Mitigating the cumulative PDG effect allows for a more robust multistage interconnected network.

VI. Conclusion

The impact of cumulative PDG in SOA-based optical multistage interconnected networks is investigated in a recirculating-loop test-bed environment that emulates the cascade of multiple switching nodes. We find that even small node PDG (0.33 dB at 1531.05 nm) can dramatically affect the OSNR degradation due to accumulated ASE noise. The maximum number of cascaded nodes was shown to vary by 10 nodes from the case where no PDG exists, depending on both the packet wavelength and its input SOP. Large node number variation translates into considerably smaller network sizes than that projected. A shortcoming of 10 nodes corresponds to a 100-fold decrease in the number of interconnected ports of an optical network such as the data vortex. The deviation in the number of cascaded nodes was found to approximately increase linearly with 34 node/1 dB of node PDG. The impact of PDG should therefore be addressed through improved SOA design with a PDG that is lower than 0.1 dB. Alternatively, optimum channel placement in the low PDG gain region is suitable for smaller network sizes. For larger network sizes, we propose the use of PM fibers between switching nodes with an alignment of the PM fiber to the SOA to compensate for the channels that experience higher PDG. This approach mitigates the effect of PDG on all three channels with a maximum cumulative PDG of 1 dB for up to 20 nodes, minimizing the shift in the maximum reach for more robust and scalable optical multistage interconnected networks.

References

[1] A. K. Kodi and A. Louri, "Design of a high-speed optical interconnect for scalable shared-memory multiprocessors," *IEEE Micro*, vol. 25, no. 1, pp. 41–49, Jan./Feb. 2005.

[2] R. Ramaswami and K. N. Sivarajan, *Optical Networks: A Practical Perspective*, 2nd ed. San Francisco, CA: Morgan Kaufmann, 2002.

[3] W. J. Dally and B. Towles, *Principles and Practices of Interconnection Networks*. San Francisco, CA: Morgan Kaufmann, 2004.

[4] Special Issue on Optical Networks, *IEEE J. Lightw. Technol.*, vol. 23, no. 10, Oct. 2005.

[5] A. Shacham, B. A. Small, O. Liboiron-Ladouceur, and K. Bergman, "A fully implemented 12 × 12 data vortex optical interconnection network," *J. Lightw. Technol.*, vol. 23, no. 10, pp. 3066–3075, Oct. 2005.

[6] I. Armstrong, I. Andonovic, and A. E. Kelly, "Semiconductor optical amplifiers: Performance and applications in optical packet switching," *J. Opt. Netw.*, vol. 3, no. 12, pp. 882–897, Nov. 2004.

[7] R. Luijten, C. Minkenberg, R. Hemenway, M. Sauer, and R. Grzybowski, "Viable opto-electronic HPC interconnect fabrics," in *Proc. ACM/IEEE SC*, Portland, OR, Nov. 2005, p. 18.

[8] K. A. Williams, G. F. Roberts, T. Lin, R. V. Penty, I. H. White, M. Glick, and D. McAuley, "Integrated optical 2 × 2 switch for wavelength multiplexed interconnects," *IEEE J. Sel. Topics Quantum Electron.*, vol. 11, no. 1, pp. 78–85, Jan./Feb. 2005.

[9] C. Tai and W. I. Way, "Dynamic range and switching speed limitations for an N × N optical packet switch based on low-gain semiconductor optical amplifiers," *J. Lightw. Technol.*, vol. 14, no. 4, pp. 525–533, Apr. 1996.

[10] O. Liboiron-Ladouceur, B. A. Small, and K. Bergman, "Physical layer scalability of a WDM optical packet interconnection network," *J. Lightw. Technol.*, vol. 24, no. 1, pp. 262–270, Jan. 2006.

[11] A. E. Kelly, C. Tombling, C. Michie, and I. Andonovic, "High performance semiconductor optical amplifier," presented at the Optical Fiber Commun. Conf., Los Angeles, CA, Mar. 2004, ThS1.

[12] P. Koonath, S. Kim, W.-J. Cho, and A. Gopinath, "Polarization-insensitive quantum-well semiconductor optical amplifiers," *IEEE J. Quantum Electron.*, vol. 38, no. 9, pp. 1282–1290, Sep. 2002.

[13] L. H. Spiekman, J. M. Wiesenfeld, A. H. Gnauck, L. D. Garrett, G. N. Van Den Hoven, T. Van Dongen, M. J. H. Sander-Jochem, and J. J. M. Binsma, "Transmission of 8 DWDM channels at 20 GB/s over 160 km of standard fiber using a cascade of semiconductor optical amplifiers," *IEEE Photon. Technol. Lett.*, vol. 12, no. 6, pp. 717–719, Jun. 2000.

[14] P. J. Winzer, M. Pfennigbauer, M. M. Strasser, and W. R. Leeb, "Optimum bandwidths for optically preamplified NRZ receivers," *J. Lightw. Technol.*, vol. 19, no. 9, pp. 1263–1273, Sep. 2001.

[15] B. F. Kennedy, S. Philippe, P. Landais, A. L. Bradley, and H. Soto, "Experimental investigation of polarisation rotation in semiconductor optical amplifiers," *Proc. Inst. Electr. Eng.—Optoelectron.*, vol. 151, no. 2, pp. 114–118, Apr. 2004.

[16] A. El Amari, N. Gisin, B. Perny, H. Zbinden, and C. W. Zimmer, "Statistical prediction and experimental verification of concatenations of fiber optic components with polarization dependent loss," *J. Lightw. Technol.*, vol. 16, no. 3, pp. 332–339, Mar. 1998.

[17] L. Q. Guo and M. J. Connelly, "Signal-induced birefringence and dichroism in a tensile-strained bulk semiconductor optical amplifier and its application to wavelength conversion," *J. Lightw. Technol.*, vol. 23, no. 12, pp. 4037–4045, Dec. 2005.

[18] C. Vinegoni, M. Karlsson, M. Petersson, and H. Sunnerud, "The statistics of polarization-dependent loss in a recirculating loop," *J. Lightw. Technol.*, vol. 22, no. 4, pp. 968–976, Apr. 2004.

[19] Y. Sun, A. O. Lima, I. T. Lima, Jr., J. Zwck, L. Yan, C. R. Menyuk, and G. M. Carter, "Statistics of the system performance in a scrambled recirculating loop with PDL and PDG," *IEEE Photon. Technol. Lett.*, vol. 15, no. 8, pp. 1067–1069, Aug. 2003.

[20] M. J. Connelly, *Semiconductor Optical Amplifiers*. London, U.K.: Kluwer, 2002.

[21] G. P. Agrawal and N. A. Olsson, "Self-phase modulation and spectral broadening of optical pulses in semiconductor laser amplifiers," *IEEE J. Quantum Electron.*, vol. 25, no. 11, pp. 2297–2306, Nov. 1989.

[22] Y. Sun, I. T. Lima, A. O. Lima, H. Jiao, J. Zweck, L. Yan, G. M. Carter, and C. R. Menyuk, "System performance variations due to partially polarized noise in a receiver," *IEEE Photon. Technol. Lett.*, vol. 15, no. 11, pp. 1548–1650, Nov. 2003.

[23] M. Shtaif and A. Mecozzi, "Polarization-dependent loss and its effect on the signal-to-noise ratio in fiber-optic systems," *IEEE Photon. Technol. Lett.*, vol. 16, no. 2, pp. 671–673, Feb. 2004.

[24] I. T. Lima, O. A. Lima, Y. Sun, H. Jiao, J. Zweck, C. R. Menyuk, and C. M. Carter, "A receiver model for optical fiber communication systems with arbitrarily polarized noise," *J. Lightw. Technol.*, vol. 23, no. 3, pp. 1478–1490, Mar. 2005.

Odile Liboiron-Ladouceur (S'95) was born in Montréal, QC, Canada. She received the B.Eng. degree in electrical engineering from the McGill University, Montréal, in 1999 and the M.S. degree in electrical engineering from the Columbia University, New York, NY, in 2003. She is currently working toward the Ph.D. degree in electrical engineering at the Columbia University.

From 1999 to 2000, she was with Teradyne Inc. as an Applications Engineer in the mass storage business unit. She then joined Texas Instruments Incorporated in 2000 and spent two years working in the fiber optic business unit as a design engineer. Her research interests include optical interconnection physical layer analysis, clock, and data recovery solutions for optical packet switching interconnection networks.

Keren Bergman (S'87–M'95) received the B.S. degree in electrical engineering from the Bucknell University, Lewisburg, PA, in 1988 and the M.S. and Ph.D. degrees in electrical engineering from the Massachusetts Institute of Technology, Cambridge, in 1991 and 1994, respectively.

She is an Associate Professor of electrical engineering at Columbia University, New York, NY. Her research interests include ultrafast optical signal processing, wavelength-division-multiplexing optical networking, and optical packet interconnection for high-performance computing.

Prof. Bergman is currently an Associate Editor of the IEEE PHOTONIC TECHNOLOGY LETTERS and the Optical Society of America (OSA) *Journal of Optical Networking*. She is a Fellow of the OSA.

Misha Boroditsky (SM'06) received the M.S. degree in applied physics from St. Petersburg Polytechnic Institute, St. Petersburg, Russia, in 1993 and the Ph.D. degree in physics from the University of California, Los Angeles, in 1999. His Ph.D. dissertation was on the modification of spontaneous emissions in photonic crystals.

After graduation, he worked for more than six years with the Optical Systems Research Department, AT&T Laboratories, on various aspects of access architectures, ultrafast optical packet switching, and polarization-mode dispersion. Since May 2006, he has been working in the field of quantitative finance with the Statistical Arbitrage Group, Knight Equity Markets, Jersey City, NJ. He has authored or coauthored more than 50 publications. He is the holder of six patents.

Dr. Boroditsky served on the Optical Fiber Communications Technical Committee from 2004 to 2006 and was the Lasers and Electro-Optics Society Meeting Committee Chair for 2005–2006.

Misha Brodsky (M'01) received the Diploma (M.Sc.) degree from St. Petersburg Technical University, St. Petersburg, Russia, in 1992 and the Ph.D. degree in physics from Massachusetts Institute of Technology, Cambridge, in 2000.

For a year, he was a Research Associate with Ioffe Institute, where he studied properties of multiple-quantum-well structures. His graduate school research was focused on the behavior of strongly correlated electrons in low-dimensional systems in the quantum Hall regime. During graduate school, he spent the summer of 1997 with Bell Labs, Murray Hill, NJ, where he worked on novel photodectors. In 2000, he joined the Optical System Research Division, AT&T Labs, Middletown, NJ, as a Senior Member of Technical Staff. He has worked in various physical-layer telecom research areas including WDM metro architectures, polarization-mode dispersion, and, more recently, quantum key distribution.

Dr. Brodsky is a member of the American Physical Society and the Optical Society of America.